CONTRIBUTIONS TO ZOOLOGY (2019) 1-29

BRILL

CTOZ
brill.com/ctoz

Does polyxenous symbiosis promote sympatric divergence? A morphometric and phylogeographic approach based on *Oxydromus okupa* (Annelida, Polychaeta, Hesionidae)

Miguel A. Meca
Centre d'Estudis Avançats de Blanes (CEAB-CSIC), Carrer d'Accés a la Cala Sant Francesc 14, 17300 Blanes (Girona), Catalunya, Spain
meca.miguelangel@gmail.com

Pilar Drake
Instituto de Ciencias Marinas de Andalucía (ICMAN-CSIC), Avenida República Saharaui 2, Puerto Real 11519, Cádiz, Spain

Daniel Martin
Centre d'Estudis Avançats de Blanes (CEAB-CSIC), Carrer d'Accés a la Cala Sant Francesc 14, 17300 Blanes (Girona), Catalunya, Spain

Abstract

The polychaete *Oxydromus okupa* lives in association with the bivalves *Scrobicularia plana* and *Macomopsis pellucida* in the intertidal of Río San Pedro (CI = Cádiz Intertidal) and adjacent to CHipiona (CH) harbour, and in the subtidal of the Bay of Cádiz (CS = Cádiz Subtidal). We analyse these populations morphometrically, ecologically (including infestation characteristics) and genetically (intertidal populations, 16S and ITS-1 genes). We consider "host", "environment" and the combined "host and environment" as possible factors of interpopulation variability. Morphometry revealed three well-defined clusters for CI, CH and CS, showing intergroup phenotypic differences ranging from 35 to 50%. Hosts shell lengths ranged between 26 and 36 mm for *S. plana* and 20 and 28 mm for *M. pellucida*. The infestation of small *M. pellucida* by juvenile *O. okupa* suggests they show an active size segregation behaviour. The intertidal seems to be less favourable (infestation rate <25% vs. up to 65% in the subtidal), and did not show recent bottleneck events. Overall, CI and CH were genetically homogeneous, but showed a significant divergence (one dominant haplotype in each host species), suggesting host shift as being a soft barrier to gene flow. Most characters related with host-entering varied among populations, suggesting symbiotic behaviour to play a key role in reducing panmixia and leading to the initial phases of a speciation process in sympatric symbiotic populations. Polyxeny and symbiotic behaviour in *O. okupa* seem thus to be underlying mechanisms contributing to its great phenotypic variety, marked ecological differences, and genetic divergence.

Keywords

Behaviour – Bivalvia – demography – evolution – *Macomopsis* – morphology – panmixia – *Scrobicularia* – symbiosis – sympatry

1 Introduction

Sympatric populations (i.e., conspecific populations with genetically based phenotypic differences that coexist spatially) are of interest in evolutionary biology, as they hold the potential of becoming a first step toward sympatric speciation. They may also be more common than hitherto thought, since they may have passed unnoticed using the number of loci typical of the pre-genomics era (Jorde et al., 2018). The rich cryptic diversity of polychaetes (Nygren, 2014) triggered an increasing number of studies focusing on sympatric populations (e.g., Nygren et al., 2010; Nygren & Pleijel, 2011; Zanol et al., 2016; Styan et al., 2017; Nygren et al., 2018). In the particular case of symbiotic polychaetes, however, polyxenous species (i.e., symbiotic species inhabiting different hosts) appear to be less pervasive than monoxenous ones (i.e., symbionts inhabiting a single host) (Martin & Britayev, 1998, 2018), while they are the most likely candidates for hidden cryptic speciation among sympatric populations. To date, the only known study on the phylogeography of symbiotic polychaetes comprised the monoxenous Mediterranean *Ophryotrocha mediterranea* Martin, Abelló & Cartes, 1991 and the polyxenous Atlantic-Mediterranean *Iphitime cuenoti* Fauvel, 1914 (Lattig et al., 2016). This study showed that polyxeny did not represent a biological barrier to gene flow among sympatric populations of the latter species that inhabit four species of brachyuran crabs.

The present study concerns a different polyxenous relationship under sympatric conditions. The aims are to assess whether host and environmental preferences affect morphology, gene flow and demography, ultimately attempting to clarify diversification mechanisms in marine invertebrate symbionts. The symbiotic hesionid polychaete *Oxydromus humesi* (Pettibone, 1961) was described as belonging to *Parasyllidea* by Pettibone (1961), based on a single population living in association with the tellinid bivalve *Austromacoma nymphalis* (Lamarck, 1818) in mangrove swamps in the Republic of Congo (Martin et al., 2015). Two populations were later reported as symbionts of bivalves, i.e., the semelid *Scrobicularia plana* (da Costa, 1778) in the intertidal of Río San Pedro and the tellinid *Macomopsis pellucida* (Spengler, 1798) in the subtidal of the Bay of Cádiz, both at the southern Atlantic coast of the Iberian Peninsula (Martin et al., 2012, 2015). The Iberian populations were finally described as belonging to a new species based on morphometric analyses, i.e., *Oxydromus okupa* Martin, Meca & Gil in Martin et al. (2017).

The population associated with *S. plana* was studied in detail in terms of behaviour, infestation characteristics, and life cycle (Martin et al., 2015, 2017). It showed a regular distribution (i.e., a single symbiont individual per host), intra-specific aggression, a complex host-entering behaviour, and low (usually <5%) and seasonally fluctuating infestations that were closely related with the reproductive cycle (e.g., males leaving their hosts during spring/summer, likely for fertilization purposes). The life cycle postulated for *O. okupa* consisted on 1) a planktonic larval phase settling on soft bottoms when competent, 2) free-living juveniles, and 3) adults able to

select (whenever possible) and enter the hosts at a given size.

In this study, we report a third population of *O. okupa*, recently discovered living intertidally in association with *M. pellucida* at Micaela Beach, adjacent to the harbour of Chipiona, ca. 40 km north-west of the Bay of Cádiz. We take this opportunity to assess the possible existence of population-level differences in morphology, gene flow, and demography. We consider two factors, host (*S. plana* vs. *M. pellucida*) and environment (subtidal vs. intertidal), as well as their combined effect (intertidal *S. plana* vs. subtidal *M. pellucida*).

Therefore, our aims are: (1) to check for variations in morphology (based on morphometry) and ecology (based on population-size structure and infestation rates); (2) to test the possible influence of host shift in gene flow, based on two fast-evolving neutral markers (i.e., 16S and ITS-1) that proved to be useful in assessing relationships amongst conspecific populations in polychaetes (Nygren, 2014); and (3) to analyse the symbiont demographic history by mismatch distribution, estimates of genetic diversity, and neutrality evolution tests (based on the two aforementioned genes). Furthermore, we are providing new sequence information on Hesionidae. Despite some recent papers (e.g., Pleijel et al., 2011, 2012; Jimi et al., 2018; Rouse et al., 2018), this information is still very scarce in relation to the high species diversity of this family, particularly for the symbiotic species.

2 Material and methods

2.1 *Sampling*

Specimens of *O. okupa* were collected from three populations of bivalve hosts in the Gulf of Cádiz: CI (Cádiz Intertidal) with *S. plana* (family Semelidae) in the intertidal of Río San Pedro; CH (CHipiona) with *M. pellucida* (family Tellinidae) in the intertidal of Micaela Beach adjacent to Chipiona harbour; CS (Cádiz Subtidal) with *M. pellucida* in the subtidal zone at the outlet of Río San Pedro in the Bay of Cádiz (fig. 1).

Materials from previous sampling belonging to CS (January 2013) and CI (April, June, July, August, September, October, November and December 2011 and January, February, March, April and May 2012) (Martin et al., 2017) were used for morphometric analyses. Additional specimens were collected in May 2016 by hand from the sediment during low tide in CH (fig. 1). Specimens for morphometry were relaxed in 7.2% magnesium chloride in distilled water, preserved in 4% seawater/formalin solution for a few days, rinsed in fresh water, and transferred to 70% ethanol. For genetic purposes, additional specimens were collected on September 2017 (CH) and on September and November 2017 and May and June 2018 (CI), and were preserved directly in 100% ethanol. Attempts to obtain DNA-grade materials from CS in October 2017 and June 2018 failed, likely due to changes in the bottom configuration in this highly dynamic region, which prevented finding any specimen in the previously surveyed area. As a result, 38 symbionts (19 from CH and 19 from CI) were available for genetics.

2.2 *Morphometry*

Morphometric analyses were based on 68 specimens (20 from CH, 23 CS, 25 from CI), all of them fixed in formalin and preserved in alcohol (as there may be significant differences in appendage measurements according to the fixation method). The following measurements were selected (following Martin et al., 2017; fig. 2): worm length (WL, μm), number of segments (NS), worm width without parapodium (WWP, μm), length of dorsal lobe (DL, μm), length of dorsal cirrophore (DCP, μm), length of dorsal cirrostyle (DCS, μm), length

FIGURE 1 Sampled localities of the host bivalves harbouring *Oxydromus okupa* in the Gulf of Cadiz region: (CI) Cádiz Intertidal (*Scrobicularia plana*); (CS) Cádiz Subtidal (*Macomopsis pellucida*); (CH) Chipiona intertidal (*M. pellucida*). Images obtained from Google Earth v. 7.3, © Google 2018.

of posterior neurochaetal lobe (PNCL, µm), length of ventral cirri (VC, µm), head width (HW, µm), head length (HL, µm), length of lateral antenna (LA, µm), length of palpophore (PP, µm), length of palpostyle (PS, µm), distance between anterior eyes (DAE, µm), distance between posterior eyes (DPE, µm) and distance between anterior and posterior eyes (DAPE, µm). The width of the tenth segment (parapodia included) was used as a proxy for worm size (WW, µm). Due to cirrostyles alternating short and long through the segments (Martin et al., 2015, 2017), all parapodial characters were measured for two parapodia (from chaetiger 10 to 30, depending on the specimen) bearing long and short cirrostyles and indicated by adding L and S to the end of the acronym (e.g., "PNCLL" and "PNCLS", meaning posterior neurochaetal lobe from parapodia having long and short cirrostyles, respectively). WW, WL, NS and WWP were measured under a Nikon SMZ645 stereomicroscope equipped with a micrometric ocular, while the rest of the characters using a Motic BA210 binocular microscope equipped with a TOUPCAM™ U3CMOS digital camera, managed by the ToupView 3.7 software.

Inter-population differences were analysed for size-independent data and taxonomically relevant character proportions modified from Martin et al. (2017) by including WL/NS, WL/WWP and NS/WWP (table 1). Size-dependency of measured characters was assessed by Pearson correlation and the resulting size-dependent ones were divided by WW. The pairwise differences among populations for the averaged measurements were estimated by one-way ANOVAs with

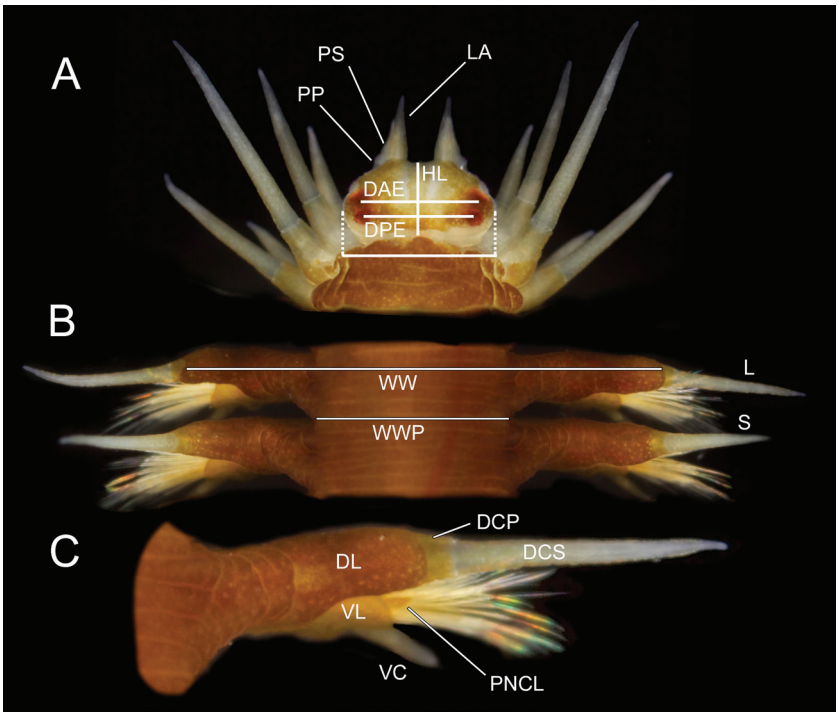

FIGURE 2 *Oxydromus okupa.* Anterior end (A), two midbody segments (B) and one mid-body parapodia (C), showing the measurements used in the morphometric analyses. WW: worm width with parapodia (µm); WWP: worm width without parapodia (µm); HW: head width (µm); HL: head length (µm); LA: length of lateral antenna (µm); PP: length of palpophore (µm); PS: length of palpostyle (µm); DAE: distance between anterior eyes (µm); DPE: distance between posterior eyes (µm); DAPE: distance between anterior and posterior eyes (µm); DL: length of dorsal lobe (µm): DCP: length of dorsal cirrophore (µm); DCS: length of dorsal cirrostyle (µm); PNCL: length of posterior neurochaetal lobe (µm); VL: ventral lobe; VC: length of ventral cirri (µm); L: long cirrostyle; S: short cirrostyle. Redrawn from Martin et al. (2015, 2017).

post hoc Tukey's honestly significant difference (HSD) by $p < 0.05$. Both character sets (i.e., size-independent and proportions) were normalised prior the analyses. Data ordination was performed by Principal Component Analysis (PCA) and the significance of the obtained clusters was assessed by one-way analysis of similarity (ANOSIM) based on Euclidean distance resemblance matrices. The contribution of each measured character to the distance within and between the three populations was implemented by the Similarity Percentages analysis (SIMPER) based on Euclidean distance. The evaluation of the morphological identity of the populations was realized by Forward Stepwise Discriminant Analysis (FSDA) on non-transformed datasets. This analysis is based on the construction of discriminant functions, which allows the differentiation of populations, and on classification matrices obtained by pairwise comparisons, which explain the membership of each individual to its corresponding population. The reliability of these classifications was assessed by cross-validating the original matrices. The variables included in the discriminant functions were selected according to the statistics F index and Wilk's Lambda

TABLE 1 Size correlations for the characters analysed in the populations of *Oxydromus okupa*. Bold characters indicate $p < 0.05$. A: Character measurements. B: Character proportions. Coeff: Pearson correlation coefficient; p: significance level; CI: *Cádiz Intertidal* (*Scrobicularia plana*); CS: Cádiz Subtidal (*Macomopsis pellucida*); CH: Chipiona intertidal (*M. pellucida*). Character abbreviations as in fig. 2

A	CH		CS		CI		B	CH		CS		CI	
	Coeff	***p***	**Coeff**	***p***	**Coeff**	***p***		**Coeff**	***p***	**Coeff**	***p***	**Coeff**	***p***
WL	**0.85**	**<0.0001**	**0.686**	**0.001**	**0.85**	**<0.0001**	WL/NS	**0.785**	**<0.0001**	**0.641**	**0.002**	**0.926**	**<0.0001**
NS	0.406	0.085	**0.546**	**0.01**	**0.74**	**<0.0001**	WL/WWP	0.343	0.151	0.207	0.369	**0.668**	**0**
WWP	**0.755**	**0.0001**	**0.846**	**<0.0001**	**0.883**	**<0.0001**	NS/WWP	-0.322	0.178	**-0.524**	**0.015**	-0.016	0.941
DLL	**0.646**	**0.002**	**0.72**	**0**	**0.872**	**<0.0001**	DCPL/DLL	-0.069	0.772	-0.062	0.779	-0.05	0.813
DCPL	0.374	0.105	**0.589**	**0.003**	**0.796**	**<0.0001**	DCSL/DLL	-0.218	0.356	**-0.437**	**0.037**	**-0.475**	**0.016**
DCSL	**0.539**	**0.014**	0.364	0.088	**0.801**	**<0.0001**	DCSL/DCPL	-0.143	0.548	-0.358	0.093	**-0.495**	**0.012**
PNCLL	**0.61**	**0.004**	-0.222	0.308	**0.904**	**<0.0001**	VCL/PNCL	-0.128	0.591	0.359	0.092	-0.236	0.257
VCL	**0.6**	**0.005**	**0.444**	**0.034**	**0.613**	**0.001**	DCPS/DLS	0.07	0.77	0.061	0.782	0.184	0.378
DLS	**0.594**	**0.006**	**0.644**	**0.001**	**0.852**	**<0.0001**	DCSS/DLS	-0.161	0.498	-0.298	0.167	**-0.475**	**0.016**
DCPS	**0.493**	**0.027**	**0.516**	**0.012**	**0.724**	**<0.0001**	DCSS/DCPS	-0.033	0.891	-0.211	0.333	**-0.428**	**0.033**
DCSS	**0.587**	**0.006**	0.343	0.108	**0.751**	**<0.0001**	VCS/PNCS	-0.22	0.351	**0.532**	**0.009**	-0.173	0.409
PNCLS	**0.544**	**0.013**	-0.226	0.299	**0.875**	**<0.0001**	HL/HW	-0.395	0.085	-0.234	0.283	**-0.607**	**0.001**
VCS	**0.545**	**0.013**	**0.567**	**0.005**	**0.646**	**0**	LA/HL	-0.009	0.971	0.044	0.85	-0.222	0.286
HW	**0.855**	**<0.0001**	**0.708**	**0**	**0.894**	**<0.0001**	PP/HL	0.195	0.411	0.2	0.373	0.325	0.113
HL	0.357	0.122	0.366	0.086	**0.471**	**0.017**	PS/HL	0.027	0.914	0.079	0.728	-0.202	0.334
LA	0.127	0.616	0.39	0.08	0.094	0.654	PS/PP	-0.237	0.329	-0.057	0.802	**-0.502**	**0.011**
PP	0.319	0.171	**0.518**	**0.014**	**0.669**	**0**	DAE/HW	-0.108	0.652	-0.329	0.125	-0.249	0.23
PS	0.214	0.38	**0.439**	**0.041**	0.113	0.591	DPE/HW	-0.032	0.892	**-0.42**	**0.046**	-0.023	0.914
DAE	**0.782**	**<0.0001**	**0.632**	**0.001**	**0.864**	**<0.0001**	DAPE/HL	0.264	0.26	-0.124	0.572	**0.722**	**<0.0001**
DPE	**0.808**	**<0.0001**	**0.639**	**0.001**	**0.869**	**<0.0001**	DAE/DPE	-0.035	0.884	0.116	0.596	-0.19	0.364
DAPE	0.363	0.115	0.271	0.211	**0.74**	**<0.0001**							

by a threshold significance level of 0.05. The first, an asymptotic approach to the Fisher's F index (named Box test), assessed the similarity of the intra-population covariance matrices, and the second, based on the Rao approach to the Wilk's Lambda test, evaluated the differences between population averaged vectors.

Pearson correlation analyses, one-way ANOVAs and discriminant analyses were carried out in XLSTAT (2015.5.01.23039, copyright by Addinsoft 1995–2016). PCA, ANOSIM and SIMPER analyses were executed with PRIMER, version 6.1.11, copyright by PRIMER-E Ltd. 2008 (Clarke & Warwick, 2001; Clarke & Gorley, 2006).

2.3 Ecology

The specimens of *S. plana* and *M. pellucida* were opened to estimate the infestation prevalence and, to define the size structure of their populations, shell lengths were measured (in mm) using callipers. The differences in size structure between symbiont and infested bivalves were analysed by one-way ANOVA, and the significance (i.e., $p < 0.05$) of the pairwise differences was assessed by post hoc Tukey's HSD. Symbiont/host size relationships were monthly checked by correlation analyses. All samples, independent of fixation method, were included in the analysis of population size structure vs. infestation characteristics.

2.4 Molecular analyses

DNA was extracted using DNAeasy Tissue Kit (Qiagen) following the protocol supplied by the manufacturer. We amplified 471–503 bp of nuclear ITS-1 with flanking regions of 18S rDNA and 5.8S rDNA, and 469–516 bp of 16S rDNA. We used ITS18SFPOLY (GAGGAAGTAAAAGTCGTAACA) and ITS5.8SRPOLY (GTTCAATGTGTCCTGCAATTC) (Pleijel et al., 2009) for the ITS-1, and 16SarL (CGCCTGTTTATCAAAAACAT) and 16SbrH (CCGGTCTGAACTCAGATCACGT) (Palumbi, 1996) for the 16S rDNA. PCRs were realised with BIOTAQ DNA Polymerase (Bioline), with 25 µl mixtures containing: 2.5 µl of NH_4 No $MgCl_2$ Bioline Reaction Buffer (final concentration of 10X), 0.5 µl of $MgCl_2$ solution (final concentration of 50 mM), 1 µl of nucleotide mix (final concentration of 10 mM each dNTP), 0.8 µl of each primer (final concentration of 10 µM), 0.15 µl of BIOTAQ DNA polymerase (5 U/µl), 1 µl of template DNA and 17.25 µl of nuclease-free water. Temperature profiles were as follow for ITS-1: 96 °C/4' – (94 °C/30" – 48 °C/30" – 72 °C/60") x 45 cycles – 72 °C/8' – Store at 8 °C, and for 16S: 96 °C/4' – (94 °C/30" – 55–59 °C/30" – 72 °C/1') x 40–45 – 72 °C/8' – Store at 8 °C. Amplified PCR products were analysed by electrophoresis in a 1.2 % p/v agarose gel stained with ethidium bromide and then sent to Macrogen Inc. facilities (Seoul, Korea) to obtain complete double strain sequences. Consensus sequences of each chain pairs were generated and edited by BioEdit v. 7.0.5.3 software (Hall, 1999) and were aligned using MAFFT online service v. 7.407 (Katoh & Standley, 2013) under the E-INS-i strategy.

For further analyses on gene flow between CH and CI, estimates of pairwise genetic differentiation (Kst, Hst and Fst) and of the number of migrators per generation (Nm) were calculated by means of DNAsp v. 6.12 (Rozas et al., 2017). Significance of Kst, Hst and Fst were assessed by performing 1,000 permutations in DNAsp for the first two and in ARLEQUIN v. 3.5 software (Excoffier & Lischer, 2010) for the last one. The genetic distance was obtained by means of Kimura 2-parameter model (Kimura, 1980) with 1,000 bootstraps in MEGA X software (Kumar et al., 2018). The haplotype geographical distribution was checked by constructing networks through the median joining network algorithm (Bandelt et al., 1999) implemented in NETWORK v. 5 (fluxus-engineering.com). The phylogenetic relationships among haplotypes was indicated in a haplotype tree constructed

using Maximum-likelihood analysis (ML) performed in MEGA X. The tree was rooted with GenBank sequences of *Nereimyra punctata* (Müller, 1778) (DQ442577.1) and *Gyptis propinqua* Marion & Bobretzky, 1875 (DQ442573.1), the analysis was run with the GTR+I model and clade support was assessed using 100 bootstrap replicates.

Historical population demography patterns for CH and CI populations were assessed by mismatch distribution, analyzing pairwise differences between haplotypes using the model of sudden expansion (Rogers & Harpending, 1992), and testing the null hypothesis of population growth in ARLEQUIN (Excoffier et al., 2005), based on the following diversity estimators: Nh (number of haplotypes), h (haplotype diversity), and π (nucleotide diversity). The patterns were also assessed by Tajima's D test (Tajima, 1989), Fu's Fs test (Fu, 1997) and R2 test (Ramos-Onsins & Rozas, 2002) implemented in DnaSP.

The ITS-1 region is highly conservative (i.e., without polymorphism) and was thus insufficiently informative. Therefore, it was not considered suitable for the purpose of this study.

3 Results

3.1 Morphometry

Size-independent data. CI and CS had a better representation of the population size range than CH (i.e., individual sizes from 1.88 to 3.44 mm in CI; from 2.00 to 3.10 in CS and from 2.10 to 2.83 in CH). Accordingly, there were no coincident size-independent characters in all three populations (table 1). For the purposes of our analyses, all them were treated as size-dependent.

The PCA plot (fig. 3A) showed clear differences between CH, CS and CI (ANOSIM, Global R: 0.55–0.381, significance level: 0.1%). The first two PCA axes explained 47.6% of the total variation, 29.3% in case of first axis (Eigenvalue = 6.15) and 18.3% for the second one (Eigenvalue = 3.84).

The intra-population average distances were 10.67% for CH, 17.70% for CS and 18.25% for CI (SIMPER). The characters that most contributed to these intra-population similarities were related with prostomium, parapodia and worm's length and width (table 2). The inter-population dissimilarities were 45.57% (CS vs. CH), 44.24% (CI vs. CH) and 49.42% (CI vs. CS). Prostomial, parapodial, and worm's length and width variables mostly contributing to these differences (table 2).

When comparing the averaged measurements, approximately one tenth were significantly different among populations (table 3). In most cases, these were prostomial, parapodial, and worm's length and width characters (table 3), which were also those included in the discriminant functions (table 4). These functions correctly classified all individuals in the three pairwise comparisons (fig. 4), with cross-validation success probabilities of 89% (CI vs. CH), 92% (CI vs. CS) and 86% (CS vs. CH).

3.2 Character proportions

Only one over the 20 character proportions analysed were positively correlated with size in CH (table 1). In CS, there were three negative and two positive size correlations (table 1). In CI, there were six negative and three positive size relationships, suggesting allometric growth in this population (table 1).

As for size-independent characters, the PCA plot based on character proportions (fig. 3B) clearly separated the three populations (ANOSIM, Global R: 0.466–0.224, significance level: 0.1%). The two first axes explained 44% of the total variation, with 24.3% in the case of the first axis (Eigenvalue = 4.85) and 19.7% for the second one (Eigenvalue = 3.95).

The intra-population average distances were 11.19% for CH, 16.99% for CS and 18.02% for CI (SIMPER). The character proportions mostly contributing to these intra-population

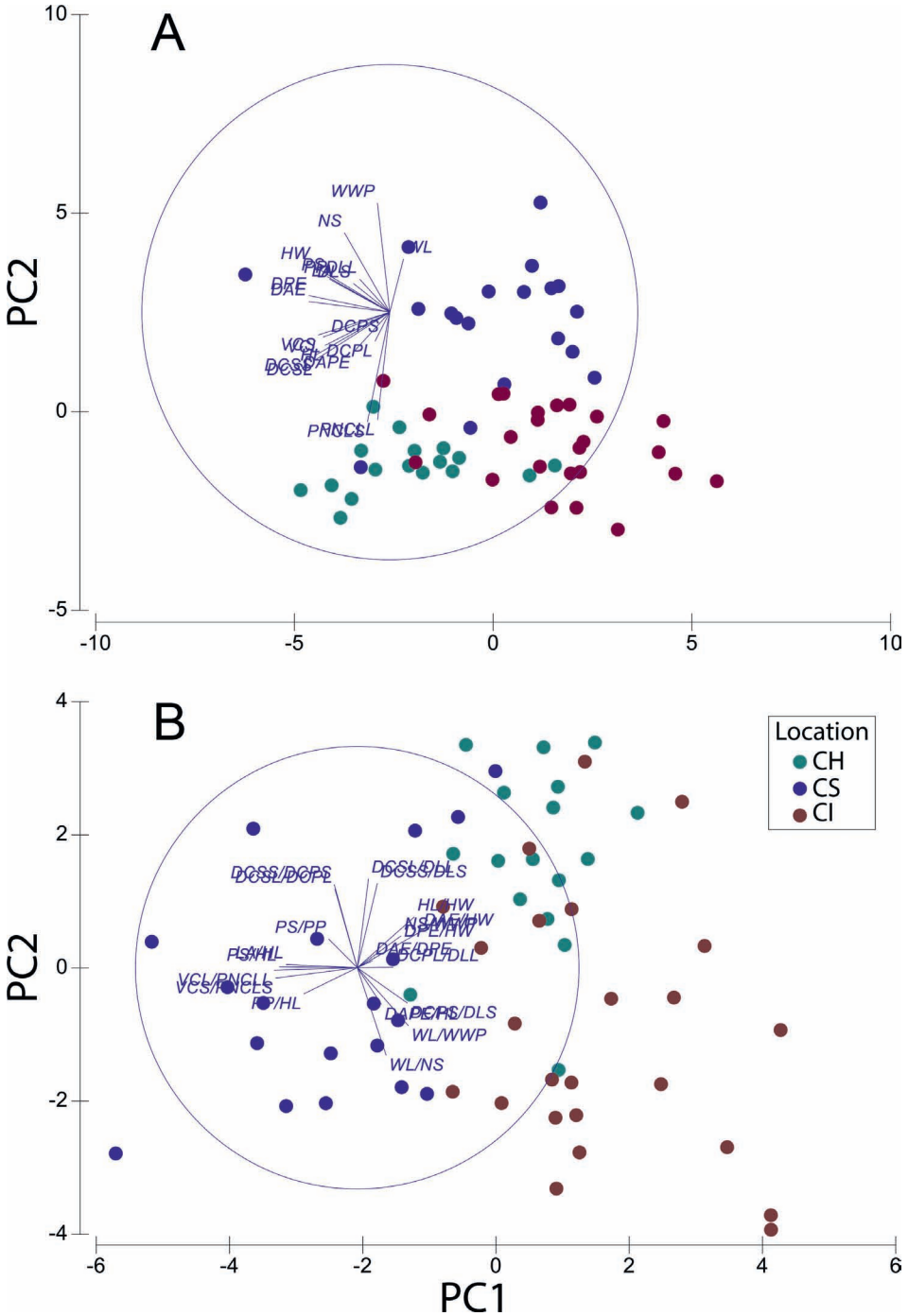

FIGURE 3 Principal Component Analyses plots. A: Based on size independent data. B: Based on character proportions. CI: Cadiz Intertidal (*Scrobicularia plana*); CS: Cadiz Subtidal (*Macomopsis pellucida*); CH: Chipiona intertidal (*M. pellucida*). Character abbreviations as in fig. 2.

TABLE 2 The six most contributing size-independent measurements to the intra-population similarities and pairwise dissimilarities among populations based on SIMPER analyses. Av. Value: Average value; Av. Sq. Dist: Average square distance; Sq. Dist/SD: Square distance divided by Standard deviation; Contrib. %: Percentage of contribution; Cum. %: Cumulative percentage of contribution. CI: *Cádiz Intertidal* (*Scrobicularia plana*); CS: Cádiz Subtidal (*Macomopsis pellucida*); CH: Chipiona intertidal (*M. pellucida*). Character abbreviations as in fig. 2

CH	**Av. Value**	**Av. Sq. Dist**	**Sq. Dist/SD**	**Contrib. %**	**Cum. %**
WL	-0.475	0.170	0.51	1.60	1.60
WWP	-0.396	0.191	0.50	1.79	3.39
PNCLL	0.719	0.195	0.50	1.83	5.22
HW	0.348	0.201	0.53	1.88	7.10
PNCLS	0.796	0.246	0.46	2.30	9.41
VCL	0.908	0.275	0.51	2.58	11.99
CS					
DCPL	-0.480	0.457	0.49	2.58	2.58
NS	0.698	0.461	0.42	2.61	5.19
WL	0.096	0.600	0.51	3.39	8.58
VCL	-0.066	0.604	0.47	3.41	11.99
WWP	1.100	0.637	0.48	3.60	15.59
DLS	0.161	0.656	0.46	3.71	19.30
CI					
PNCLS	0.352	0.164	0.45	0.90	0.90
PNCLL	0.395	0.227	0.48	1.25	2.14
DCSL	-0.519	0.407	0.47	2.23	4.38
WWP	-0.593	0.446	0.48	2.45	6.82
DCSS	-0.559	0.456	0.44	2.50	9.32
PP	-0.486	0.623	0.49	3.41	12.73

CS/CH	**CS Av. Value**	**CH Av. Value**	**Av. Sq. Dist**	**Sq. Dist/SD**	**Contrib. %**	**Cum. %**
PNCLS	-1.160	0.796	4.68	1.47	10.27	10.27
PNCLL	-1.140	0.719	4.35	1.35	9.54	19.82
DCSL	-0.356	1.130	3.25	0.93	7.13	26.95
WWP	1.100	-0.396	3.03	0.99	6.65	33.60
DCSS	-0.290	1.110	2.97	0.91	6.52	40.12
DAPE	-0.410	0.060	2.39	0.78	5.24	45.35

CI/CH	**CI Av. Value**	**CH Av. Value**				
DCSS	-0.559	1.110	3.57	1.12	8.08	8.08
DCSL	-0.519	1.130	3.47	1.08	7.84	15.92
VCL	-0.591	0.908	3.39	0.92	7.66	23.58
VCS	-0.615	0.911	3.35	1.00	7.57	31.16
DLS	-0.417	0.408	2.56	0.66	5.78	36.94
WL	0.261	-0.475	2.36	1.03	5.34	42.27

TABLE 2 The six most contributing size-independent measurements to the intra-population similarities and pairwise dissimilarities among populations based on SIMPER analyses. Av. Value: Average value; Av. Sq. Dist: Average square distance; Sq. Dist/SD: Square distance divided by Standard deviation; Contrib. %: Percentage of contribution; Cum. %: Cumulative percentage of contribution. CI: *Cádiz Intertidal* (*Scrobicularia plana*); CS: Cádiz Subtidal (*Macomopsis pellucida*); CH: Chipiona intertidal (*M. pellucida*). Character abbreviations as in fig. 2. (*cont.*)

CI/CS	CI Av. Value	CS Av. Value	Av. Sq. Dist	Sq. Dist/SD	Contrib. %	Cum. %
WWP	-0.593	1.100	3.91	0.99	7.90	7.90
PNCLL	0.395	-1.140	3.28	1.24	6.64	14.55
HW	-0.621	0.473	3.12	0.70	6.31	20.86
NS	-0.510	0.698	3.10	0.83	6.28	27.14
PNCLS	0.352	-1.160	3.07	1.43	6.21	33.35
PS	-0.413	0.383	2.60	0.72	5.25	38.60

TABLE 3 Pairwise differences based on character measurements expressed as percentages. Bold characters indicate significantly high differences (Tukey's HSD test, $p < 0.05$). CI: Cádiz Intertidal (*Scrobicularia plana*); CS: Cádiz Subtidal (*Macomopsis pellucida*); CH: Chipiona intertidal (*M. pellucida*). Character and measurement abbreviations as in fig. 2

	CS vs. CH		CI vs. CH		CI vs. CS	
Size-Independent	***p***	**Difference**	***p***	**Difference**	***p***	**Difference**
WL	0.190	7	0.051	9	0.843	2
NS	**0.031**	**6**	0.242	-2	**<0.0001**	**-9**
WWP	**<0.0001**	**11**	0.616	-2	**<0.0001**	**-13**
DLL	0.653	-2	0.117	-5	0.504	-3
DCPL	0.262	-4	0.492	4	**0.015**	8
DCSL	**<0.0001**	**-13**	**<0.0001**	**-15**	0.734	-2
PNCLL	**<0.0001**	**-26**	0.230	-4	**<0.0001**	**22**
VCL	**0.002**	**-9**	**<0.0001**	**-14**	0.091	-6
DLS	0.718	-2	**0.023**	**-6**	0.126	-4
DCPS	0.251	-6	0.970	-2	0.297	4
DCSS	**<0.0001**	**-13**	**<0.0001**	**-16**	0.439	-3
PNCLS	**<0.0001**	**-29**	0.054	-5	**<0.0001**	**24**
VCS	**0.002**	-8	**<0.0001**	**-14**	0.054	-6
HW	0.904	1	**0.003**	**-5**	**<0.0001**	**-5**
HL	**0.016**	**-7**	**0.031**	**-6**	0.902	1
LA	0.451	4	0.516	-4	**0.045**	**-8**
PP	0.977	0	**0.029**	**-7**	**0.013**	**-7**
PS	0.754	2	0.153	-6	**0.023**	**-8**
DAE	0.251	-2	**0.008**	**-4**	0.312	-2
DPE	0.540	-2	**0.009**	**-4**	0.119	-3
DAPE	0.323	-5	0.753	2	0.061	7

TABLE 4 The five most contributing size-independent and proportion characters to the inter-population discrimination in base of discriminant analyses, arranged in a decreasing order according to their contribution to intra-similarity (F index) and inter-dissimilarity (Wilk's Lambda). F: Fisher's F index; Lambda: Rao approach to the Wilk's Lambda test; *p:* significance level for both F index and Wilk's Lambda; Coeff: Standardized coefficients for the variables included in the inter-population discriminant function; CS, CH, CI: Coefficients of the selected variables in the classification functions for CS, CH and CI. Intercept: Intercept of the classification functions for each population (CS, CH and CI). CI: Cádiz Intertidal (*Scrobicularia plana*); CS: Cádiz Subtidal (*Macomopsis pellucida*); CH: Chipiona intertidal (*M. pellucida*). Character abbreviations as in fig. 2

Size-indep.	F	Lambda	*p*	Coeff	CS	CH	Proportions	F	Lambda	*p*	Coeff	CS	CH
Intercept					-572.428	-596.528	Intercept					306007.634	304182.892
PNCLS	74.320	0.314	<0.0001	0.093	-101.458	-58.037	VCS/PNCLS	32.561	0.511	<0.0001	1.031	1011.355	999.320
PNCLL	66.660	0.338	<0.0001	0.433	302.194	511.806	DAE/HW	29.737	0.533	<0.0001	-10.623	756375.854	753908.109
WWP	48.743	0.411	<0.0001	-0.188	695.680	667.270	VCL/PNCLL	20.487	0.624	<0.0001	-0.188	163.152	165.136
DCSL	36.224	0.484	<0.0001	1.547	-422.353	-178.471	DCSS/DLS	14.702	0.698	0.001	1.153	-3086.378	-3057.369
DCSS	33.537	0.503	<0.0001	-0.743	1054.612	932.342	LA/HL	13.561	0.709	0.001	-1.890	5410.569	5362.465
					CI	CH						CI	CH
Intercept					-202.839	-233.696	Intercept					215765.790	216260.947
DCSL	71.075	0.354	<0.0001	-0.537	205.944	100.487	DCSL/DCPL	51.130	0.433	<0.0001	0.280	-534.487	-533.798
DCSS	70.473	0.356	<0.0001	1.904	-197.627	178.179	WL/NS	21.341	0.646	<0.0001	4.196	9.763	10.176
VCS	44.582	0.467	<0.0001	0.428	-730.650	-551.423	DAPE/HL	17.250	0.693	0.000	-1.044	-22674.997	-22851.607
VCL	38.248	0.505	<0.0001	-0.085	828.514	795.943	DCSS/DLS	14.878	0.724	0.000	-0.656	-1835.935	-1845.865
HW	19.823	0.663	<0.0001	2.340	-593.812	413.148	VCL/PNCLL	14.056	0.735	0.001	0.182	1495.832	1499.422
					CI	CS						CI	CS
Intercept					-226.849	-247.122	Intercept					230829.783	232203.978
PNCLS	58.500	0.412	<0.0001	0.128	178.100	248.576	VCS/PNCLS	56.790	0.419	<0.0001	0.812	132.079	141.326
WWP	57.171	0.418	<0.0001	0.678	531.284	632.264	VCL/PNCLL	41.985	0.494	<0.0001	-0.045	664.082	663.610
PNCLL	52.808	0.437	<0.0001	-0.527	926.915	642.831	DAE/HW	31.370	0.597	<0.0001	-9.903	571029.157	573077.568
HW	18.249	0.692	0.000	1.802	-11259.451	-7241.627	WL/WWP	21.207	0.659	<0.0001	-1.906	48.874	45.621
NS	12.754	0.763	0.001	3.018	354.631	1320.889	WL/NS	17.220	0.704	0.000	0.361	-4.733	-4.694

FIGURE 4 Scatterplots for individual scores and centroids of the discriminant functions obtained in each pairwise comparison (i.e., CS/CH, CI/CH and CI/CS) by the discriminant analyses realized on the two data sets: size-independent data and character proportions. CI: Cádiz Intertidal (*Scrobicularia plana*); CS: Cádiz Subtidal (*Macomopsis pellucida*); CH: Chipiona intertidal (*M. pellucida*).

similarities were related with prostomial and parapodial regions, as well as with worm's length and width (table 5). The inter-population dissimilarities were 40.62% (CS vs. CH), 37.54% (CI vs. CH), and 51.68% (CI vs. CS), with proportions of prostomial, parapodial and worm's length and width characters mostly contributing to these differences (table 5).

Most averaged proportions differing significantly between populations (table 6) were mostly prostomial, parapodial, and worm's length and width characters, and were also included in the discriminant functions (table 4). These functions correctly classified all individuals in the three pairwise comparisons (fig. 4). The cross-validation success probabilities were 94% (CI vs. CH), 93% (CI vs. CS) and 78% (CS vs. CH).

3.3 Population-size structure and infestation characteristics

Over the 106 worms analysed, 62 were found in *M. pellucida* (CH = 39, CS = 23) and 44 in *S. plana*. The infestation prevalence was 0.4% (September 2017), 3.6% (November 2017), 6.7% (May 2018) and 12.5% (June 2018) in CI, and 10.2% (May 2016) and 11.4% (September 2017) in CH. However, it reached 22.2% in hosts of >20 mm length in CH, and was 66.7% (January 2013), reaching 89.3% in hosts >20 mm long in CS (January 2013).

Sizes of the symbionts ranged from 0.96 to 3.44 mm (0.96 to 2.83 mm in CH, 2.00 to 3.10 mm in CS, 1.10 to 3.44 mm in CI). Small worms were better represented in September 2017 at CH (42.11% of worms <2.00 mm, but up to 31.58% for worms <1.60 mm; fig. 8A, C) and in May 2018 at CI (85.71% of worms <2.00 mm and 57.14% <1.60 mm). In November 2017 only one symbiont was <1.60 mm at CI (fig. 8B) and no juveniles (<1.60 mm) were found at CS. Symbiont sizes were significantly smaller at CH than at CI (Tukey's HSD test, $p < 0.003$) and CS (Tukey's HSD test, $p < 0.001$), likely due to an overall major presence of juveniles. No significant difference in symbiont sizes were

TABLE 5 The six proportions most contributing to the intra-population similarities and pairwise dissimilarities among populations based on SIMPER analyses. Av. Value: Average value; Av. Sq. Dist: Average square distance; Sq. Dist/SD: Square distance divided by Standard deviation; Contrib. %: Percentage of contribution; Cum. %: Cumulative percentage of contribution. CI: Cádiz Intertidal (*Scrobicularia plana*); CS: Cádiz Subtidal (*Macomopsis pellucida*); CH: Chipiona intertidal (*M. pellucida*). Character abbreviations as in fig. 2

CH	**Av. Value**	**Av. Sq. Dist**	**Sq. Dist/SD**	**Contrib. %**	**Cum. %**
VCS/PNCLS	-0.296	0.062	0.50	0.55	0.55
VCL/PNCLL	-0.213	0.086	0.46	0.77	1.32
PS/HL	-0.313	0.321	0.48	2.87	4.19
WL/WWP	-0.231	0.331	0.51	2.96	7.15
DAE/HW	0.377	0.351	0.47	3.14	10.29
WL/NS	-0.507	0.369	0.39	3.30	13.59
CS					
WL/WWP	-0.612	0.256	0.42	1.50	1.50
WL/NS	-0.428	0.557	0.52	3.28	4.78
DCPL/DLL	-0.443	0.561	0.50	3.30	8.08
DPE/HW	-0.632	0.630	0.50	3.70	11.79
PP/HL	0.577	0.673	0.49	3.96	15.75
DCPS/DLS	-0.402	0.680	0.50	4.00	19.75
CI					
VCS/PNCLS	-0.668	0.175	0.46	0.97	0.97
VCL/PNCLL	-0.655	0.198	0.47	1.10	2.07
DCSL/DCPL	-0.691	0.327	0.41	1.81	3.88
DCSS/DCPS	-0.440	0.606	0.48	3.36	7.25
DAE/HW	0.480	0.688	0.44	3.82	11.06
DAPE/HL	0.568	0.722	0.49	4.00	15.07
CS/CH	**CS Av. Value**	**CH Av. Value**	**Av. Sq. Dist**	**Sq. Dist/SD**	**Contrib. %**	**Cum. %**
VCS/PNCLS	1.110	-0.296	3.00	0.98	7.39	7.39
DCSS/DLS	-0.383	0.736	2.78	0.82	6.85	14.24
VCL/PNCLL	1.020	-0.213	2.77	0.76	6.82	21.06
DAE/HW	-0.944	0.377	2.74	0.85	6.75	27.81
LA/HL	0.660	-0.441	2.62	0.82	6.44	34.25
DCSL/DLL	-0.335	0.635	2.48	0.89	6.11	40.36
CI/CH	**CI Av. Value**	**CH Av. Value**				
DCSL/DCPL	-0.691	0.841	3.24	0.96	8.64	8.64
WL/NS	0.698	-0.507	2.78	0.96	7.41	16.05
DAPE/HL	0.568	-0.564	2.73	0.82	7.27	23.31
WL/WWP	0.648	-0.231	2.38	0.94	6.33	29.64
DCSS/DCPS	-0.440	0.511	2.32	0.80	6.18	35.82
DCPL/DLL	0.534	-0.259	2.32	0.65	6.17	41.99

TABLE 5 The six proportions most contributing to the intra-population similarities and pairwise dissimilarities among populations based on SIMPER analyses. Av. Value: Average value; Av. Sq. Dist: Average square distance; Sq. Dist/SD: Square distance divided by Standard deviation; Contrib. %: Percentage of contribution; Cum. %: Cumulative percentage of contribution. CI: Cádiz Intertidal (*Scrobicularia plana*); CS: Cádiz Subtidal (*Macomopsis pellucida*); CH: Chipiona intertidal (*M. pellucida*). Character abbreviations as in fig. 2. (*Cont.*)

CI/CS	CI Av. Value	CS Av. Value	Av. Sq. Dist	Sq. Dist/SD	Contrib. %	Cum. %
VCS/PNCLS	-0.668	1.110	4.29	1.09	8.31	8.31
VCL/PNCLL	-0.655	1.020	4.16	0.88	8.05	16.36
DAE/HW	0.480	-0.944	3.36	0.79	6.49	22.86
WL/WWP	0.648	-0.612	3.12	0.97	6.04	28.89
PS/HL	-0.285	0.640	2.81	0.69	5.45	34.34
WL/NS	0.698	-0.428	2.77	0.89	5.37	39.71

TABLE 6 Pairwise differences based on proportions expressed as percentages. Bold characters indicate significantly high differences (Tukey's HSD test, $p < 0.05$). CI: Cádiz Intertidal (*Scrobicularia plana*); CS: Cadiz Subtidal (*Macomopsis pellucida*); CH: Chipiona intertidal (*M. pellucida*). Character abbreviations as in fig. 2

	CS vs. CH		CI vs. CH		CI vs. CS	
Proportions	***p***	**Difference**	***p***	**Difference**	***p***	**Difference**
WL/NS	0.955	1	**<0.0001**	**11**	**0.000**	**10**
WL/WWP	0.375	-5	**0.005**	9	**<0.0001**	**14**
NS/WWP	**0.036**	**-6**	0.471	-3	0.275	3
DCPL/DLL	0.817	-2	**0.022**	**10**	**0.003**	**12**
DCSL/DLL	**0.008**	**-11**	**0.019**	**-9**	0.860	2
DCSL/DCPL	**0.021**	**-8**	**<0.0001**	**-18**	**0.004**	**-10**
VCL/PNCLL	**<0.0001**	**21**	**<0.0001**	**-11**	**<0.0001**	**-31**
DCPS/DLS	0.521	-5	0.387	5	**0.035**	**10**
DCSS/DLS	**0.001**	**-11**	**0.004**	**-9**	0.821	2
DCSS/DCPS	0.388	-6	**0.006**	**-14**	0.155	-8
VCS/PNCLS	**<0.0001**	**24**	0.169	-9	**<0.0001**	**-32**
HL/HW	**0.003**	**-7**	0.769	-1	**0.011**	**6**
LA/HL	**0.002**	**11**	0.700	3	**0.007**	**-9**
PP/HL	**0.025**	**8**	1.000	0	**0.012**	**-8**
PS/HL	**0.008**	**10**	0.995	0	**0.005**	**-9**
PS/PP	0.872	2	0.976	1	0.943	-1
DAE/HW	**<0.0001**	**-3**	0.907	0	**<0.0001**	**3**
DPE/HW	**0.025**	**-2**	0.817	0	**0.002**	**2**
DAPE/HL	0.468	3	**0.001**	**-8**	**0.016**	**5**
DAE/DPE	0.453	-1	0.952	0	0.575	1

detected between CI and CS (Tukey's HSD test, $p = 0.925$).

Altogether, 401 specimens of *M. pellucida* (362 from CH and 39 from CS) and 615 of *S. plana* were collected. Length in *M. pellucida* ranged from 15.10 to 27.58 mm in CH and from 18.12 to 28.07 mm in CS. The greatest proportions of shells <20 mm were found in September 2017 at CH (67.47%) and in January 2013 at CS (39.29%). Although the number of small hosts was not insignificant in some months, most infested bivalves showed intermediate sizes (i.e., 20–28 mm). In *S. plana*, the size-class range was larger (i.e., 20.50–41.17 mm) and most infested hosts were considerably longer (i.e., 26–36 mm) than in *M. pellucida*. In fact, the size of the infested bivalves differed significantly among localities harbouring different hosts (i.e., CI vs. CH, CI vs. CS; Tukey's HSD test, $p < 0.001$), whilst there were no significant differences between CS and CH (Tukey's HSD test, $p = 0.254$).

There were significant host-symbiont size correlations observed when some specimens of *O. okupa* occurred in small *M. pellucida* bivalves. For instance, in January 2013 (Pearson coefficient = 0.400, $p = 0.021$) and in September 2017 (Pearson coefficient = 0.908, $p < 0.0001$). In turn, in May 2016, the small-sized bivalves were scarce and the relationship was non-significant (Pearson coefficient = 0.233, $p = 0.338$). As for *S. plana*, the size correlations with *O. okupa* were non-significant for all months (i.e., September and November 2017, May and June 2018, Pearson coefficient = 0.316 to 0.480, $p = 0.245$ to 0.191).

3.3 Genetics

Nuclear data. Nineteen ITS-1 sequences were obtained for CH and CI, which showed a unique haplotype (GenBank accession number: MK831008) in the 441 bp of the final alignment data set. Accordingly, this highly conservative gene did not show polymorphism.

Mitochondrial data. Nineteen 16S sequences have been obtained for CH and CI, which showed seven haplotypes (GenBank accession numbers: MK831001 – MK831007) and six polymorphic sites in the 493 bp of the final alignment data set. Among these, five were parsimony-informative. There were six haplotypes with five polymorphic positions (four parsimony-informative) in CH, and four haplotypes with three polymorphic (only one parsimony-informative) in CI. Haplotype diversity was intermediate too high in both localities, but lower in CI, whereas nuclear diversity was low, also lower in CI (table 7). The haplotype network showed two dominant haplotypes separated by one mutational step, one more frequent in *M. pellucida* at CH and another in *S. plana* at CI (fig. 5). Each main haplotype had few derived ones with low frequencies, occurring in one or two specimens and differing from the dominant one in one or two mutational steps. Three of the low-frequency

TABLE 7 Diversity measures (h and π), statistics of differentiation (Kst and Hst), fixation index (Fst) and Kimura two-parameter (K2P) distance for populations of *Oxydromus okupa* based on 16S data. In parenthesis is represented the Nm for Fst. Significant *p*-values for Kst, Hst and Fst by $p < 0.05$ indicated in bold. N: Number of individuals; Nh: Number of haplotypes; h: Haplotype diversity; π: nucleotide diversity; CI: Cádiz Intertidal (*Scrobicularia plana*); CH: Chipiona intertidal (*Macomopsis pellucida*)

Population	N	Nh	h	π	Kst	Hst	Fst	K2P
CH	19	6	0.6550 ± 0.1115	0.0026 ± 0.0019	**0.0712**	**0.0763**	**0.1298 (1.68)**	0.0023 ± 0.0012
CI	19	4	0.5906 ± 0.0882	0.0014 ± 0.0013				
Entire	38	7	0.6743 ± 0.0506	0.0022 ± 0.0016				

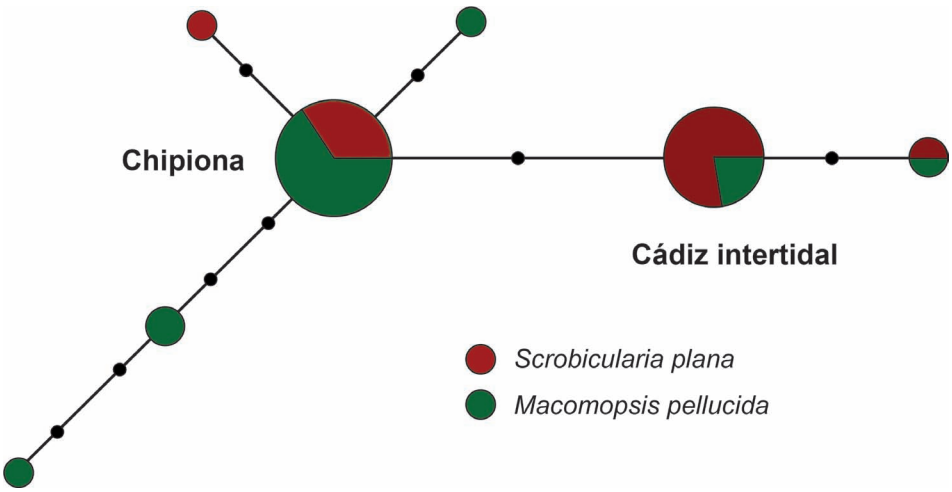

FIGURE 5 Median-joining haplotype network of mtDNA 16S sequences for *Oxydromus okupa* in relation with its host bivalves. Black points represent mutational steps. Circle and pie size are proportional to the haplotype frequency.

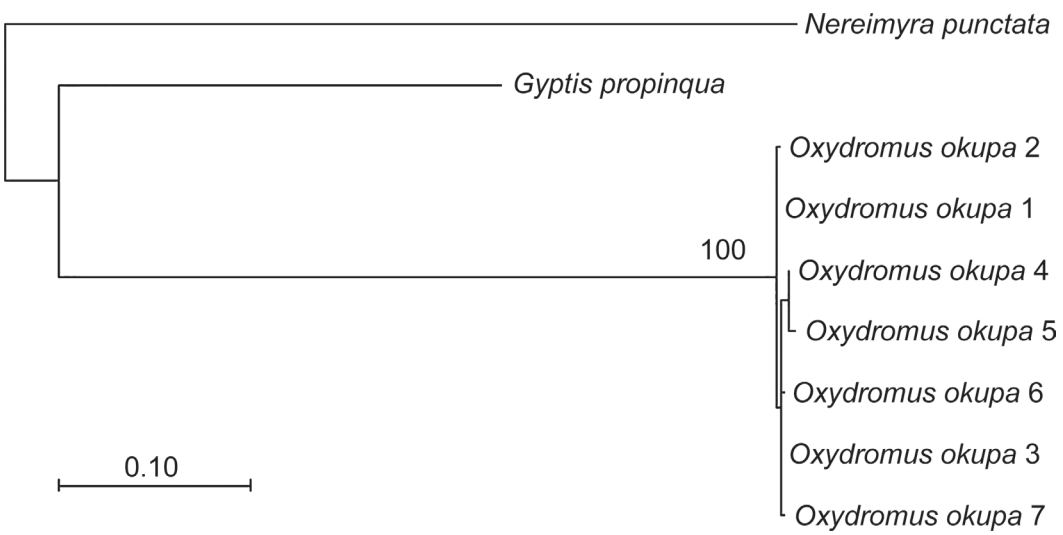

FIGURE 6 Maximum-likelihood tree of 16S haplotype data. Bootstrap values for node support >75 are represented on the corresponding branches.

haplotypes only occurred in *M. pellucida* and only one in *S. plana.* The dominant haplotypes (and their respective derivatives) have frequencies of 68% (*M. pellucida* at CH) and 75% (*S. plana* at CI).

The haplotype tree showed a single, highly supported clade (100% bootstrap) including the seven haplotypes present in the symbiont (fig. 6). Two subgroups were also identified, one of them including the dominant

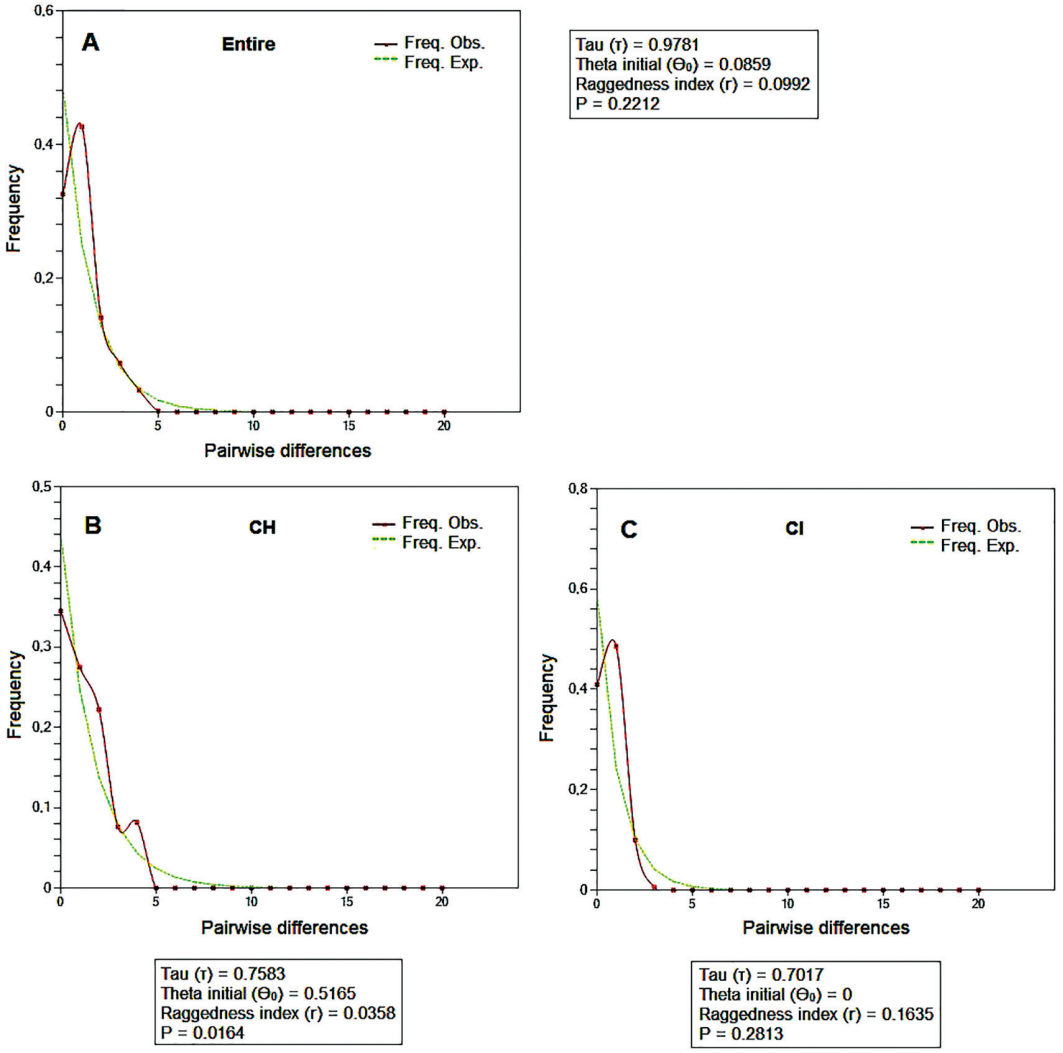

FIGURE 7 Mismatch distributions for populations of *Oxydromus okupa* for 16S data. The x-axis represents the number of pairwise differences among sequences; the y-axis shows the frequency of the pairwise comparisons. A, graph for the whole metapopulation. B, Graph for CH. C, Graph for CI. CI: Cádiz Intertidal (*Scrobicularia plana*); CH: Chipiona intertidal (*Macomopsis pellucida*).

M. pellucida haplotype at CH with its four derivatives, but with a low support (bootstrap <50%). Therefore, no well-defined lineages can be established in *O. okupa*, as supported by its low divergence (K2P distance = 0.2%). However, this variability in 16S seems to be enough to differentiate the populations, both at the levels of nucleotides (Kst > 0.05 and significant) and haplotypes (Hst > 0.05 and significant). Accordingly, the significant Fst (>0.1) together with the Nm = 1.68 suggest that this differentiation was caused by a restricted panmixia. Mismatch distributions show that most sequences either differ in one position

TABLE 8 Neutrality tests and its corresponding *p*-values in base of 16S for the two populations of *Oxydromus okupa* altogether and individually. CI: Cádiz Intertidal (*Scrobicularia plana*); CH: Chipiona intertidal (*Macomopsis pellucida*)

Population	N	Tajima's D	D p	Fu's Fs	Fs p	R2	R2 p
CH	19	-0.3385	0.4340	-16.225	0.1114	0.1252	0.2623
CI	19	-0.4961	0.3140	-0.8594	0.1820	0.1310	0.2766
Entire	38	-0.6880	0.3050	-21.448	0.0951	0.0884	0.2531

(42.7%) or did not differ (32.6%), highlighting the great inter-individual genetic homogeneity (fig. 7A). Pairwise differences were more evenly distributed in CH (no differences = 34.5%, one position = 27.5%, two positions = 22.2%) (fig. 7B) than in CI (no differences = 40.9%, one position = 48.5%) (fig. 7C). The low values of the mismatch distribution parameters (τ and Θ_0) also confirmed this high genetic homogeneity in the populations of *O. okupa* (fig. 7). The raggedness index was low and non-significant for the mismatch distributions of the entire sample and for CI (fig. 7A, C), as indicated by the observed fitting with the expected distributions. However, the non-significant neutrality tests (table 8) allow rejecting the hypothesis of sudden expansion, and support a neutral pattern of evolution and a long-term stable demography for the studied populations.

4 Discussion

During the last two decades, different morphometric approaches attempted to discriminate species boundaries in polychaete cryptic and pseudo-cryptic species complexes (e.g., Omena & Amaral, 2001; Ford & Hutchings, 2005; Garraffoni et al., 2006; Lattig et al., 2007; Hernández-Alcántara & Solís-Weiss, 2014; Coutinho et al., 2015; Martin et al., 2017). However, none of them used a combination of morphometrics and genetics to evaluate differentiation levels between populations under different sources of variation, including host-symbiont relationships, a perspective that falls within the framework of integrative taxonomy (Will et al., 2005; Padial et al., 2010; Giribet, 2015; Martin et al., 2017). Our data support that *O. okupa* is a genuine polyxenous symbiont showing a high phenotypical and ecological plasticity, which is translated into a local divergence (both morphometrical and ecological). The species also shows an inter-population genetic substructure, which could be affected by a combination of gene flow barriers (e.g., host and habitat) in sympatric conditions.

4.1 *Morphological and ecological divergence*

The inter-population morphometric dissimilarities in *O. okupa* ranged from 35 to 50% and were always higher when comparing CS vs. CI. This suggests that the two levels of inter-population differentiation may be acting as sources of evolution, with the combination of both host and habitat seeming to play the major role. Particularly, when we consider proportions, the difference between CS and CI is 1.4 times higher than those between CH and CS and CI. The adaptive character of this divergence cannot be currently assessed. However, the complex host-entering behaviour showed by the population infesting *S. plana*, together with the presence of a free-living phase in the life-cycle of the symbiont

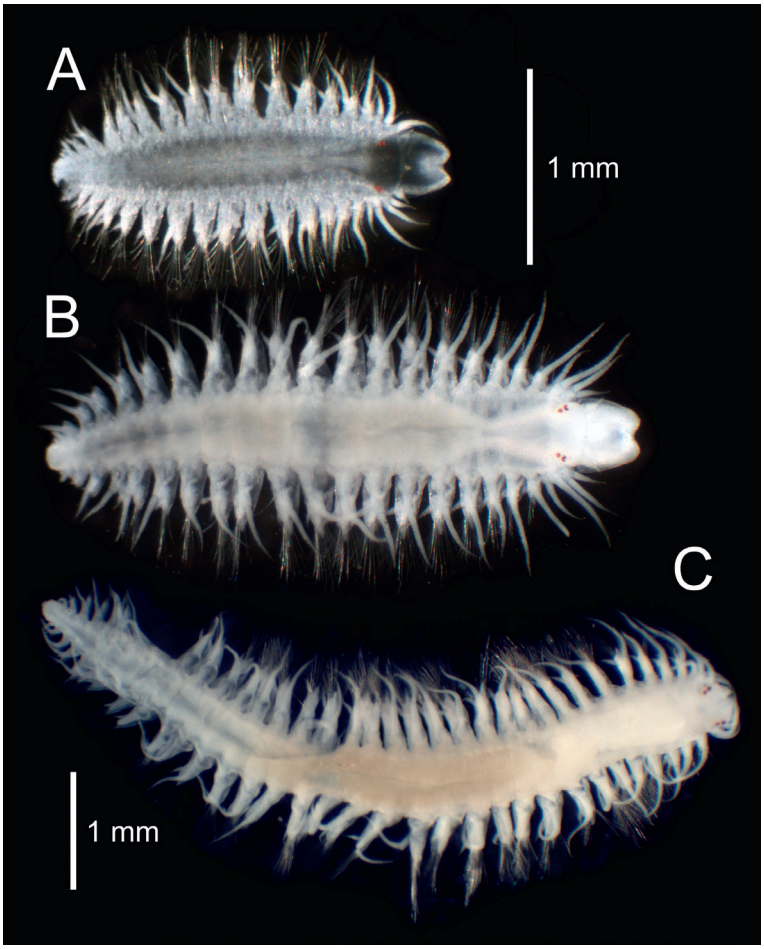

FIGURE 8 Juvenile phases of *Oxydromus okupa*. A: The smallest exemplar collected in the study (0.96 mm long) at CH. B: A juvenile (1.10 mm long) found at CI. C: A juvenile (1.54 mm long) collected at CH.

(Martin et al., 2017), lead us to expect that host and habitat might be able to affect worm shape. The cephalic region is the first body part that contacts the host's inhalant siphon during the entering process. Accordingly, the characters and proportions that contribute most to the differentiation in the studied populations are related to the prostomium, but also to the parapodia and to the length and width of the symbionts (tables 2–6).

The ecological differences between the studied localities were accompanied by differences in infestation characteristics and size structure of both the host and symbiont populations, which support the different host and environment preferences as drivers for the observed variability. Symbionts infesting *M. pellucida* were able to occupy host individuals of <28 mm shell length, whilst those hosted by *S. plana,* usually occurred in hosts of 26–36 mm shell length. Thus, the symbiont population size range was more restricted when it was associated with *M. pellucida* than with *S. plana*. On the other hand, the subtidal seems

to be the most favourable habitat, showing infestations 12 times higher than the intertidal (67% vs. 5.5%, respectively). However, a significant representation of juvenile symbionts was only found at CH in September 2017 and at CI in May 2018. In turn, the positive size correlations between *O. okupa* and *M. pellucida* found when small bivalves were available (i.e., September 2017 in CH and January 2013 in CS) suggests that not only *O. okupa* adults but also juveniles (likely coming from a free-living phase) may infest bivalves with small sizes (i.e., <20 mm). However, this seemed not to occur frequently, as infestation in small hosts was always lower than that in large adults. The high percentage of *O. okupa* juveniles at CI in May 2018 contrasts with their practically total absence in all remaining periods (only one juvenile found in the 17 months sampled in CI, including this study and that by Martin et al., 2017). This suggests that juveniles may show relevant concentrations also in larger bivalves under certain conditions, such as the absence of small hosts or a predominance of small-sized symbionts in the population. Nevertheless, it must be taken into account that the available information for CH and CS is punctual and refers to different periods of the year. Thus, a more complete data set (particularly in terms of seasonal representativeness) would certainly be required to confirm our hypotheses.

The level of morphometric differentiation between *O. okupa* and the congeneric *O. humesi* was close to 50% according to Martin et al. (2017). In this case, the sources of variation postulated were host (*S. plana* vs. *A. nymphalis*, respectively) and biogeographical distribution (Iberian Peninsula *vs*. Congo, respectively). Our study reveals a similar morphometric difference at the inter-population level in *O. okupa*. In fact, these differences are even higher than those previously reported for most sibling species described on the basis of morphometry (e.g., Coutinho et al., 2015; Ford & Hutchings, 2005). However, molecular data (Fst, K2P distance and haplotype network and tree) support that the divergence observed among the Iberian populations appears to be restricted to a local level. As available material for molecular analyses of the Congolese population is lacking, we agree that it belongs to a different, sibling species. Moreover, contrary to what occurs among the Iberian populations, it should be noted that the length of dorsal and ventral parapodial lobes consistently differs between Iberian and Congolese specimens (Martin et al., 2017), this being a classical taxonomic character allowing distinction of species within the Hesionidae (Pleijel, 1998; Ruta et al., 2007).

4.2 *Sources of evolution*

Host shifts have been considered major drivers for diversification in animal symbionts with high dispersal capacity, including marine symbionts with planktonic, potentially highly dispersive larvae (Clayton et al., 2016; Horká et al., 2016). Moreover, we suggest that environmental shifts might also act as a key driver for the variability observed in symbiotic species with free-living juvenile or early-adult phases. To date, animal symbionts most studied in terms of divergence caused by their symbiotic mode of life are parasitic insects like fleas, mites or louses (Whiting et al., 2008; Bruyndonckx et al., 2009; Bush et al., 2016; Doña et al., 2017) and phytoparasites like aphids, beetles or nematodes (Messina, 2004; Picard et al., 2007; Bass et al., 2013). These groups are highly abundant and diverse in terrestrial ecosystems and, particularly in the case of phytoparasites, host/parasite evolutionary relationships may play a key role in the emergence of new crop pests.

As for marine environments, numerous studies focused on the role of oceanographic barriers to regulate gene flow both in invertebrates and fish (e.g., Palero et al., 2008; Galarza et al., 2009; Marie et al., 2016). Conversely, similar studies dealing with the role of oceanographic and biological barriers (i.e., host type) in symbionts are very scarce and dealt with animal residents in corals or sponges (Duffy, 1996; Faucci et al., 2007; Hoeksema et al., 2018). Moreover, there is a single one dealing with symbiotic polychaetes (Lattig et al., 2016). Considering this poor background on evolutionary relationships in marine invertebrate symbionts, our work represents the first documented case of host and environment preferences as a source of variation in symbiotic polychaetes and one of the first for marine invertebrate symbionts.

When a symbiotic population shifts to a new host or to a new environment, the organisms may assume local adaptations providing specialised responses to the new conditions, even without restriction of gene flow, if the selective pressure is sufficient (Nosil, 2008; Edelaar et al., 2012). Specialization may then be followed by a genetic structuration in case of reduced intra-population gene flow, leading to lineage diversification. In case of sufficient and persistent isolation, the evolutionary autonomy of one of these lineages will lead to a speciation event. Accordingly, we differentiate four stages in the symbiont divergence process mediated by host and environment shifts, which may start after a basal stage in which the symbionts colonize a new host or environment (stage 0). These are: (1) local variations/adaptations with gene flow, (2) local variations/adaptations with reduction of gene flow, (3) lineage differentiation, (4) evolutionary lineage autonomy leading to speciation. However, we also presume that: (1) this general scheme may show variations depending on each particular case, and (2) the relative extent of each step may be strongly dependent on the symbiont and host biological traits, as well as on the selective pressure imposed by the host and environment preferences.

The morphometric and ecological differences found between the populations of *O. okupa* seem to indicate a specialised response to the particular conditions they support (both in terms of host and environment), together with a present situation of limited panmixia. In fact, our 16S data indicate that such a divergence may occur with a significant restriction of gene flow (significant values of Kst, Hst and Fst, and $Nm < 2$), indicating a moderately advanced speciation process (i.e., stage 2). In addition, the observed genetic substructure would be the agent leading to the emergence of two dominant haplotypes, one at CH (with three exclusive derivatives) and another one at CI, separated by one mutational step (fig. 5). However, this single mutational step, together with the low bootstrap support for the clades and the low genetic distance between localities, seems not to have allowed the establishment of two well-defined lineages within the species. Therefore, host shift seems to be a soft barrier for gene flow in *O. okupa*, probably due to the high similarity in morphology and in the mode of life of the two host bivalves. In a similar way, the substructure found in the populations of the phyllodocid polychaete *Pterocirrus giribeti* Leiva & Taboada, 2018 in Leiva et al. (2018) was attributed to an oceanic front that limited gene flow only during the species reproduction periods (i.e., a soft barrier) (Leiva et al., 2018). However, whilst this is a physical soft barrier, it is certainly biological (i.e., host shift) in the case of *O. okupa*.

The mechanisms leading host preferences to affect panmixia are unknown, but it is expected that a specialised behaviour in a symbiont may be relevant. This is the case of the population of *O. okupa* associated with

S. plana (Martin et al., 2015). The worm uses the anterior-most region to manipulate the inhalant siphon of the bivalve in order to induce its complete widening and accessibility, to enter through it, and to finally settle in the host's mantel cavity. *Scrobicularia plana* has non indented shell borders and therefore it needs to fully open the two valves in order to enable the siphons to stick out above the substrate. In *M. pellucida,* the siphons may protrude through its indented shell borders without opening the valves, while the existence of a complex mechanism has not been observed in the associated symbionts (an observation that merits further study). However, some behavioural variation may be expected, as our morphometric data show that the cephalic appendix related with host entering (together with some parapodial and, less directly, worm length and width characters) differed among the populations associated to the two hosts. This may certainly play a key role as selective pressure for the respective populations of *O. okupa.* On the other hand, chemically mediated cues driving juvenile settlement (either generated by the host or by the own adult symbionts) seem to be widespread among symbiotic polychaetes (Martin & Britayev, 1998, 2018). Thus, we may expect different chemically-mediated host-recognition mechanisms for the two bivalve hosts involved in relationships with *O. okupa*, this being an additional evolutionary driver. This may be particularly relevant if we assume that only worms able to detect and subsequently enter in one particular bivalve species would be able to contribute to the population gene pool (another interesting hypothesis to be tackled in future studies). Therefore, in light of our data, we hypothesize that symbiotic behaviour may play a key role in triggering speciation processes in the spatially coexisting populations of *O. okupa* and, thus, in sympatric populations of polyxenous symbiotic species in general.

4.3 Demographic history and genetic diversity

Despite the low infestation rates at CH (~10% and fluctuant) and CI (usually <5%), both populations did not depart from a neutral evolution model (table 8). Therefore, we may assume a long-term stable demography for the species, without indications of recent bottleneck events. There may be other non-registered populations in Cádiz Bay, which may be in contact with those studied here (Martin et al., 2017), with CH and CI being redoubts of the overall distribution of *O. okupa* around the nearby biogeographic region. Anyway, although our finding of the population at CI indirectly supports this idea, the existence of these hypothetical locations remains unproven. The populations studied here are characterized by having an intermediate to high haplotype and low nucleotide diversities, giving rise to a high level of genetic homogeneity. This is also well represented in the mismatch distributions both for the whole metapopulation and for each individual population, indicating the existence of very few intra- and inter-populations differences (fig. 7A–C). Despite the postulated homogeneous gene flow in *O. okupa*, CH significantly differed from CI (in terms of Kst, Hst, Fst and haplotype network), and was slightly more genetically diverse, both in haplotype and nucleotide diversity. We may assume that this could be related to the first being more susceptible to recruitment than the second. Accordingly, CH showed an overall higher number of juveniles than CI. Nevertheless, as indicated above, a more extended survey, both in terms of time and space, is required to confirm this hypothesis.

5 Conclusions

The populations of *O. okupa* have a great internal morphological similarity, while they

vary from 35 to 50% amongst each other and remain clearly discriminated based on different statistical analyses (i.e., PCA, ANOSIM, SIMPER, FSDA).

Oxydromus okupa seems to occupy shells of different sizes depending on the host species, which may be related with the different size structure of the native populations of the two host bivalves. The shell length of the infested *S. plana* usually ranges between 26 and 36 mm, while in *M. pellucida* it mostly ranges between 20 and 28 mm. In this sense, the higher number of small hosts in *M. pellucida* appears to be related to the high representation of juvenile symbionts at CH, suggesting an active size segregation behaviour in *O. okupa*. Furthermore, the intertidal zone seems to be the least favourable habitat for the symbiont as reflected by the low infestation rates found there.

The populations at CH and CI lived in association with two different host species and showed an overall genetic homogeneity, but with a significant differentiation in terms of Kst, Hst, Fst and Nm. This allows us to suggest that host preferences, even in the case of these two closely related hosts may act as a soft barrier to gene flow.

The morphology of body parts most related with the host entering process (i.e., the worm's cephalic and parapodial appendages) varied among populations. Accordingly, we suggest that symbiotic behaviour may be an important mechanism affecting panmixia and triggering speciation among sympatric populations.

In spite of the low infestation in intertidal habitats, both CH and CI populations did not present signs of bottleneck events and revealed to be long-term stable (in accordance with neutrality tests). This suggests a hypothetical connection through unknown populations from the Gulf of Cádiz (Martin et al., 2017).

In summary, polyxeny and symbiotic behaviour in *O. okupa* seem to be underlying mechanisms contributing to its great phenotypic variety and marked ecological differences, as well as to the observed genetic divergence.

Acknowledgements

This study derives from the "Treball de Fi de Màster" (TFM) of the author, which entitle him to obtain the MSc degree at the University of Barcelona. It is also a contribution to the Consolidated Research Group on Marine Benthic Ecology of the "Generalitat de Catalunya" (2017SGR378) and to the Research Project PopCOmics (CTM2017–88080), funded by the Spanish "Agencia Estatal de Investigación" (AEI) and the European Regional Development Fund (FEDER). The authors would like to thank Dr Arne Nygren for the helpful discussions on the molecular techniques and Drs Marta Pascual and Ferran Palero for their support with the phylogeographical approach, and to the latter also for reviewing the molecular sections. Dr Chiara Romano and the Molecular Service of the CEAB, particularly Gustavo Carreras, kindly helped us with the molecular analyses. The authors would also like to thank Dr Chris Glasby, an anonymous reviewer and the editor, Dr Bert Hoeksema, for their comments, which highly contributed to the quality of the paper.

References

Bandelt, H.J., Forster, P. & Röhl, A. (1999) Median-joining networks for inferring intraspecific phylogenies. *Mol. Biol. Evol.*, 16, 37–48.

Bass, C., Zimmer, C.T., Riveron, J.M., Wilding, C.S., Wondji, C.S., Kaussmann, M., Field, L.

M., Williamson, M.S. & Nauen, R. (2013) Gene amplification and microsatellite polymorphism underlie a recent insect host shift. *Proc. Nat. Acad. Sci. USA*, 110, 19460–19465.

Bruyndonckx, N., Dubey, S., Ruedi, M. & Christe, P. (2009) Molecular cophylogenetic relationships between European bats and their ectoparasitic mites (Acari, Spinturnicidae). *Mol. Phylogenet. Evol.*, 51, 227–237.

Bush, S.E., Weckstein, J.D., Gustafsson, D.R., Allen, J., DiBlasi, E., Shreve, S.M., Boldt, R., Skeen, H.R. & Johnson, K.P. (2016) Unlocking the black box of feather louse diversity: a molecular phylogeny of the hyper-diverse genus *Brueelia*. *Mol. Phylogenet. Evol.*, 94, 737–751.

Clayton, D.H., Bush, S.E. & Johnson, K.P. (2016) *Coevolution of Life on Hosts: Integrating Ecology and History*. University of Chicago Press, Chicago, IL.

Clarke, K.R. & Gorley, R.N. (2006) *PRIMER v6: User Manual/Tutorial* (*Plymouth Routines in Multivariate Ecological Research*). PRIMER-E Ltd, Plymouth.

Clarke, K.R. & Warwick, R.M. (2001) *Change in Marine Community: An Approach to Statistical Analysis and Interpretation,* 2nd edition. Plymouth: PRIMER-E Ltd.

Coutinho, M.C.L., Paiva, P.C. & Santos, C.S.G. (2015) Morphometric analysis of two sympatric species of *Perinereis* (Annelida: Nereididae) from the Brazilian coast. *J. Mar. Biol. Ass. UK,* 95, 953–959.

Da Costa, E.M. (1778) *Historia Naturalis Testaceorum Britanniae or The British Conchology; Containing the Description and other Particulars of Natural History of the Shells of Great Britain and Ireland*. Millan, White, Elmsley & Robson, London.

Doña, J., Sweet, A.D., Johnson, K.P., Serrano, D., Mironov, S. & Jovani, R. (2017) Cophylogenetic analyses reveal extensive host-shift speciation in a highly specialized and host-specific symbiont system. *Mol. Phylogenet. Evol.*, 115, 190–196.

Duffy, J.E. (1996) Resource-associated population subdivision in a symbiotic coral-reef shrimp. *Evolution*, 50, 360–373.

Edelaar, P., Alonso, D., Lagerveld, S., Senar, J.C. & Björklund, M. (2012) Population differentiation and restricted gene flow in Spanish crossbills: not isolation-by-distance but isolation-by-ecology. *J. Evol. Biol.*, 25, 417–430.

Excoffier, L., Laval, G. & Schneider, S. (2005) Arlequin (version 3.0): an integrated software package for population genetics data analysis. *Evol. Bioinf. Online,* 1, 47–50.

Excoffier, L. & Lischer, H.E. (2010) Arlequin suite ver 3.5: a new series of programs to perform population genetics analyses under Linux and Windows. *Mol. Ecol. Res.*, 10, 564–567.

Faucci, A., Toonen, R.J. & Hadfield, M.G. (2007) Host shift and speciation in a coral-feeding nudibranch. *Proc. R. Soc. London. B: Biol. Sci.*, 274, 111–119.

Fauvel, P. (1914) Un Eunicien énigmatique *Iphitime cuenoti* n. sp. *Archiv. Zool. Expér. Gén.,* 53, 34–37.

Ford, E. & Hutchings, P. (2005) An analysis of morphological characters of *Owenia* useful to distinguish species: description of three new species of *Owenia* (Oweniidae: Polychaeta) from Australian waters. *Mar. Ecol.,* 26, 181–196.

Fu, Y.X. (1997) Statistical tests of neutrality of mutations against population growth, hitchhiking and background selection. *Genetics*, 147, 915–925.

Galarza, J.A., Carreras-Carbonell, J., Macpherson, E., Pascual, M., Severine, R., Turner, G. F. & Rico, C. (2009) The influence of oceanographic fronts and early-life-history traits on connectivity among littoral fish species. *Proc. Nat. Acad. Sci. USA*, 106, 1473–1478.

Garraffoni, A.R.S. & de Garcia Camargo, M. (2006) First application of morphometrics in a study of variations in uncinial shape present within the Terebellidae (Polychaeta). *Zool. Stud.,* 45, 75–80.

Giribet, G. (2015) Morphology should not be forgotten in the era of genomics – a phylogenetic

perspective. *Zool. Anz. – A. J. Comp. Zool.*, 256, 96–103.

Hall, T.A. (1999) BioEdit: a user-friendly biological sequence alignment editor and analysis program for Windows 95/98/NT. *Nucleic Acids Symp. Ser.* (*Oxf.*), 41, 95–98.

Hernández-Alcántara, P. & Solís-Weiss, V. (2014) Anatomical and morphometric analysis of a new species of *Leitoscoloplos* (Annelida Orbiniidae) with numerous stomach papillae, from the Gulf of California, Eastern Pacific. *Contrib. Zool.*, 83, 133–105.

Hoeksema, B.W., Butôt, R. & García-Hernández, J.E. (2018) A new host and range record for the gall crab *Fungicola fagei* as a symbiont of the mushroom coral *Lobactis scutaria* in Hawai'i. *Pac. Sci.*, 72, 251–262.

Horká, I., De Grave, S., Fransen, C.H.J.M., Petrusek, A. & Ďuriš, Z. (2016) Multiple host switching events shape the evolution of symbiotic palaemonid shrimps (Crustacea: Decapoda). *Sci. Rep.*, 6, 26486.

Jimi, N., Eibye-Jacobsen, D. & Salazar-Vallejo, S.I. (2018) Description of *Elisesione imajimai* sp. nov. from Japan (Annelida: Hesionidae) and a redescription of *E. problematica* (Wesenberg-Lund, 1950) and its confirmation within hesionini. *Zool. Stud.*, 57, 8.

Jorde, P.E., Andersson, A., Ryman, N. & Laikre, L. (2018) Are we underestimating the occurrence of sympatric populations? *Mol. Ecol.*, 27, 4011–4025.

Katoh, K. & Standley, D.M. (2013) MAFFT multiple sequence alignment software version 7: improvements in performance and usability. *Mol. Biol. Evol.*, 30, 772–780.

Kimura, M. (1980) A simple method for estimating evolutionary rates of base substitutions through comparative studies of nucleotide sequences. *J. Mol. Evol.*, 16, 111–120.

Kumar, S., Stecher, G., Li, M., Knyaz, C. & Tamura, K. (2018) MEGA X: Molecular Evolutionary Genetics Analysis across computing platforms. *Mol. Biol. Evol.*, 35, 1547–1549.

Lamarck, J.B. (1818) *Histoire naturelle des Animaux sans Vertèbres, présentant les caractères généraux et particuliers de ces animaux, leur distribution, leurs classes, leurs familles, leurs genres, et la citation des principales espèces qui s'y rapportent; précédée d'une introduction offrant la détermination des caractères essentiels de l`animal, sa distinction du végétal et des autres corps naturels, enfin, l'exposition des principes fondamentaux de la zoologie*. Déterville & Verdière, Paris.

Lattig, P., San Martín, G. & Martin, D. (2007) Taxonomic and morphometric analyses of the *Haplosyllis spongicola* complex (Polychaeta: Syllidae: Syllinae) from Spanish seas, with redescription of the type species and descriptions of two new species. *Sci. Mar.,* 71, 551–570.

Lattig, P., Muñoz, I., Martin, D., Abelló, P. & Machordom, A. (2016) Comparative phylogeography of two symbiotic dorvilleid polychaetes (*Iphitime cuenoti* and *Ophryotrocha mediterranea*) with contrasting host and bathymetric patterns. *Zool. J. Linn. Soc.*, 179, 1–22.

Leiva, C., Riesgo, A., Avila, C., Rouse, G.W. & Taboada, S. (2018) Population structure and phylogenetic relationships of a new shallow-water Antarctic phyllodocid annelid. *Zool. Scr.*, 47, 714–726.

Marie, A.D., Lejeusne, C., Karapatsiou, E., Cuesta, J.A., Drake, P., Macpherson, E., Bernatchez, L. & Rico, C. (2016) Implications for management and conservation of the population genetic structure of the wedge clam *Donax trunculus* across two biogeographic boundaries. *Sci. Rep.*, 6, 39152.

Marion, A.F. & Bobretzky, N. (1875) Étude des annélides du Golfe de Marseille. *Ann. Sci. Nat.,* 6, 1–106.

Martin, D., Abelló, P. & Cartes, J. (1991) A new species of *Ophryotrocha* (Polychaeta: Dorvilleidae) commensal in *Geryon longipes* (Crustacea: Brachyura) from the Western Mediterranean Sea. *J. Nat. Hist.,* 25, 279–291.

Martin, D. & Britayev, T.A. (1998) Symbiotic polychaetes: review of known species. *Oceanogr. Mar. Biol. Ann. Rev.,* 36, 217–340.

Martin, D. & Britayev, T.A. (2018) Symbiotic polychaetes revisited: an update of the known species and relationships (1998–2017). *Oceanogr. Mar. Biol. Ann. Rev,* 56, 367–446.

Martin, D., Cuesta, J.A., Drake, P., Gil, J., Nygren, A. & Pleijel, F. (2012) The symbiotic hesionid *Parasyllidea humesi* Pettibone, 1961 (Annelida: Polychaeta) hosted by *Scrobicularia plana* (da Costa, 1778) (Mollusca: Bivalvia: Semelidade) in European waters. *Org. Divers. Evol.*, 12, 145–153.

Martin, D., Meca, M.A., Gil, J., Drake, P. & Nygren, A. (2017) Another brick in the wall: population dynamics of a symbiotic species of *Oxydromus* (Annelida, Hesionidae), described as new based on morphometry. *Contrib. Zool.,* 83, 181–211.

Martin, D., Nygren, A., Hjelmstedt, P., Drake, P. & Gil, J. (2015) On the enigmatic symbiotic polychaete '*Parasyllidea*' *humesi* Pettibone, 1961 (Hesionidae): taxonomy, phylogeny and behaviour. *Zool. J. Linn. Soc.*, 174, 429–446.

Messina, F.J. (2004) Predictable modification of body size and competitive ability following a host shift by a seed beetle. *Evolution*, 58, 2788–2797.

Müller, O.F. (1788) Zoologia *Danica seu animalium Daniae et Norvegiae rariorum ac minus notorum descriptiones et historia.* N. Möller, Copenhague.

Nosil, P. (2008) Speciation with gene flow could be common. *Mol. Ecol.*, 17, 2103–2106.

Nygren, A., Eklöf, J. & Pleijel, F. (2010) Cryptic species of *Notophyllum* (Polychaeta: Phyllodocidae) in Scandinavian waters. *Org. Divers. Evol.*, 10, 193–204.

Nygren, A. & Pleijel, F. (2011) From one to ten in a single stroke–resolving the European *Eumida sanguinea* (Phyllodocidae, Annelida) species complex. *Mol. Phylogenet. Evol.*, 58, 132–141.

Nygren, A. (2014) Cryptic polychaete diversity: a review. *Zool. Scr.*, 43, 172–183.

Nygren, A., Parapar, J., Pons, J., Meißner, K., Bakken, T., Kongsrud, J.A., Oug, E., Gaeva, D., Sikorski, A., Johansen, R.A., Hutchings, P.A., Lavesque, N. & Capa, M. (2018) A mega-cryptic species complex hidden among one of the most common annelids in the North East Atlantic. *PLoS ONE*, 13, e0198356.

Omena, E.P. & Amaral, A.C.Z. (2001) Morphometric study of the nereidid *Laeonereis acuta* (Annelida: Polychaeta). *J. Mar. Biol. Ass. U.K.,* 81, 423–426.

Padial, J.M., Miralles, A., De la Riva, I. & Vences, M. (2010) The integrative future of taxonomy. *Front. Zool.*, 7, 16.

Palero, F., Abelló, P., Macpherson, E., Gristina, M. & Pascual, M. (2008) Phylogeography of the European spiny lobster (*Palinurus elephas*): influence of current oceanographical features and historical processes. *Mol. Phylogenet. Evol.*, 48, 708–717.

Palumbi, S.R. (1996) Nucleic acids II: the polymerase chain reaction. In: D.M. Hillis, C. Moritz & B.K. Mable (Eds) *Molecular Systematics*, 2nd edition, pp. 205–247. Sinauer, Sunderland.

Pettibone, M.H. (1961) New species of polychaete worms from the Atlantic Ocean, with a revision of the Dorvilleidae. *Proc. Biol. Soc. Wash.*, 74, 167–186.

Pleijel, F. (1998) Phylogeny and classification of Hesionidae (Polychaeta). *Zool. Scr.*, 27, 89–163.

Pleijel, F., Rouse, G. & Nygren, A. (2009) Five colour morphs and three new species of *Gyptis* (Hesionidae, Annelida) under a jetty in Edithburgh, South Australia. *Zool. Scr.*, 38, 89–99.

Pleijel, F., Rouse, G.W. & Nygren, A. (2011) A revision of *Nereimyra* (Psamathini, Hesionidae, Aciculata, Annelida). *Zool. J. Linn. Soc.*, 164, 36–51.

Pleijel, F., Rouse, G.W., Sundkvist, T. & Nygren, A. (2012) A partial revision of *Gyptis* (Gyptini, Ophiodrominae, Hesionidae, Aciculata, Annelida), with descriptions of a new tribe, a new genus and five new species. *Zool. J. Linn. Soc.*, 165, 471–494.

Picard, D., Sempere, T. & Plantard, O. (2007) A northward colonisation of the Andes by the potato

cyst nematode during geological times suggests multiple host-shifts from wild to cultivated potatoes. *Mol. Phylogenet. Evol.*, 42, 308–316.

Ramos-Onsins, S.E. & Rozas, J. (2002) Statistical properties of new neutrality tests against population growth. *Mol. Biol. Evol*, 19, 2092–2100.

Rogers, A.R. & Harpending, H. (1992) Population growth makes waves in the distribution of pairwise genetic differences. *Mol. Biol. Evol.*, 9, 552–569.

Rouse, G.W., Carvajal, J.I. & Pleijel, F. (2018) Phylogeny of Hesionidae (Aciculata, Annelida), with four new species from deep-sea eastern Pacific methane seeps, and resolution of the affinity of *Hesiolyra*. *Invertebr. Syst.*, 32, 1050–1068.

Rozas, J., Ferrer-Mata, A., Sánchez-DelBarrio, J.C., Guirao-Rico, S., Librado, P., Ramos-Onsins, S.E. & Sánchez-Gracia, A. (2017) DnaSP 6: DNA sequence polymorphism analysis of large data sets. *Mol. Biol. Evol.*, 34, 3299–3302.

Ruta, C., Nygren, A., Rousset, V., Sundberg, P., Tillier, A., Wiklund, H. & Pleijel, F. (2007) Phylogeny of Hesionidae (Aciculata, Polychaeta), assessed from morphology, 18S rDNA, 28S rDNA, 16S rDNA and COI. *Zool. Scr.,* 36, 99–107.

Spengler, L. (1798) Over det toskallede Slægt Tellinerne. *Skriv. Nat.-Selsk, Kiøbenh.,* 4, 67–121.

Styan, C.A., McCluskey, C.F., Sun, Y. & Kupriyanova, E.K. (2017) Cryptic sympatric species across the Australian range of the global estuarine invader *Ficopomatus enigmaticus* (Fauvel, 1923) (Serpulidae, Annelida). *Aquat. Invasions*, 12, 53–65.

Tajima, F. (1989) Statistical method for testing the neutral mutation hypothesis by DNA polymorphism. *Genetics*, 123, 585–595.

Whiting, M.F., Whiting, A.S., Hastriter, M.W. & Dittmar, K. (2008) A molecular phylogeny of fleas (Insecta: Siphonaptera): origins and host associations. *Cladistics*, 24, 677–707.

Will, K.W., Mishler, B.D. & Wheeler, Q.D. (2005) The perils of DNA barcoding and the need for integrative taxonomy. *Syst. Biol.*, 54, 844–851.

Zanol, J., da Silva, T.D.S. & Hutchings, P. (2016) *Marphysa* (Eunicidae, polychaete, Annelida) species of the *sanguinea* group from Australia, with comments on pseudo-cryptic species. *Invertebr. Biol.*, 135, 328–344.

RECEIVED: 19 DECEMBER 2018 | REVISED AND ACCEPTED: 5 APRIL 2019

EDITOR: B.W. HOEKSEMA